AIP | Journal of Applied Physics

Characterization of wavelet coefficients for ultrasonic signals

Jongeun Choi and Jung-Wuk Hong

Citation: J. Appl. Phys. **107**, 114909 (2010); doi: 10.1063/1.3429087
View online: http://dx.doi.org/10.1063/1.3429087
View Table of Contents: http://jap.aip.org/resource/1/JAPIAU/v107/i11
Published by the American Institute of Physics.

Additional information on J. Appl. Phys.

Journal Homepage: http://jap.aip.org/
Journal Information: http://jap.aip.org/about/about_the_journal
Top downloads: http://jap.aip.org/features/most_downloaded
Information for Authors: http://jap.aip.org/authors

ADVERTISEMENT

Downloaded 19 Apr 2013 to 143.248.118.125. This article is copyrighted as indicated in the abstract. Reuse of AIP content is subject to the terms at: http://jap.aip.org/about/rights_and_permissions

Characterization of wavelet coefficients for ultrasonic signals

Jongeun Choi[1] and Jung-Wuk Hong[2,a)]
[1]*Department of Mechanical Engineering, Michigan State University, Michigan 48824, USA*
[2]*Department of Civil and Environmental Engineering, Michigan State University, Michigan 48824, USA*

(Received 21 November 2009; accepted 18 April 2010; published online 14 June 2010)

A wavelet transform has been widely used to investigate the characteristics of wave signals for a decade. However, only qualitative investigation of the spectrogram was made rather than a quantitative interpretation. On the other hand, an analytical closed-form representation of the wavelet transformed wave signal can be used as a basis function in estimating parameters using nonlinear least-squares optimization. We derived a quantitative closed-form equation directly from the analytical continuous wavelet transformation of a pulse with a Gaussian spectrum. A fundamental three-dimensional shape of a wavelet in the spectrogram was obtained, and the analytical form was compared quantitatively with numerical results. © *2010 American Institute of Physics*. [doi:10.1063/1.3429087]

I. INTRODUCTION

A wavelet transform is an integration procedure superposing a specific wavelet function over a given signal with scaling and shifting a mother wavelet. The wavelet expansion and transformation have been used widely in the signal processing since the wavelet expansion coefficients represent local temporal characteristics while Fourier coefficients provide the energy spread over all the time domain.[1–3] Many kinds of wavelets such as Haar, Mexican hat, and Morlet have been developed, and each wavelet was chosen for the specific purpose of the application such as signal and image processing, wave analysis,[4–7] and material evaluation.[8–12]

Traditionally, the evaluation of ultrasonic signals have been the most important and fundamental task in understanding the wave traveling in a medium, and the wavelet transform has been used for many years[13–15] to explain the evolution of waves forms. However, only qualitative explanation such as the center frequency and the distribution patterns of the wavelet spectrograms was achieved so far rather than quantitative investigation.[16]

Numerically computed wavelet transformed signals have been often used for investigating unknown parameters.[17–19] However, to estimate parameters using nonlinear least-squares estimation[20] or to perform the optimal design of experiments[21] with least estimation errors in terms of D-, A-, E-, and T-optimality, the analytical closed-form solution of the wavelet transformed signal has to be obtained. To meet the needs in the aforementioned areas, we derived a closed-form solution of the acoustic signal transformed to wavelet domain, and verified the derived equation with numerical examples.

II. THEORY

Let an acoustic echo have the characteristic of a Gaussian distribution in the frequency domain with a mean value μ and a standard deviation σ, of the form

$$\hat{x}(\omega) = \frac{1}{\sigma\sqrt{2\pi}} e^{-(\omega-\mu)^2/2\sigma^2}, \tag{1}$$

where $\hat{x}(\omega)$ is the Fourier transform of a pulse $x(t)$. It can be easily shown that $\omega_c = \mu$ and $B = 2\sigma$ so that the magnitude of the spectrum has a center frequency ω_c and a bandwidth B in the form of

$$\hat{x}(\omega) = \frac{2}{B\sqrt{2\pi}} e^{-2(\omega-\omega_c)^2/B^2}, \tag{2}$$

and the inverse Fourier transform is defined as

$$x(t) = \frac{1}{2\pi}\int_{-\infty}^{\infty} \hat{x}(\omega) e^{j\omega t} d\omega. \tag{3}$$

Substituting Eq. (2) to Eq. (3) and integrating, we have

$$x(t) = \frac{1}{2\pi} e^{-j\omega_c t} e^{-B^2 t^2/8}. \tag{4}$$

With the time shift t_c from the origin, a waveform which has a Gaussian spectrum signal is expressed as

$$x(t) = \frac{1}{2\pi} e^{j\omega_c (t-t_c)} e^{-B^2 (t-t_c)^2/8}. \tag{5}$$

Using Eq. (5), a Gaussian-spectrum pulse signal with the spectral characteristics of the center frequency ω_c, the bandwidth B, and the time delay t_c can be represented conveniently. A wavelet shown in Fig. 1(a) is made from the spectral distribution in Fig. 1(b) where the center frequency f_c is 6.0 MHz, the bandwidth B_f is 4.0 MHz, and the time delay t_c is 2.5 μsec.

A. Continuous wavelet transform

The continuous wavelet transform of a signal $x(t)$ is defined in a convolution form as[1]

a)Electronic mail: jwh@egr.msu.edu.

 © 2010 American Institute of Physics

Downloaded 19 Apr 2013 to 143.248.118.125. This article is copyrighted as indicated in the abstract. Reuse of AIP content is subject to the terms at: http://jap.aip.org/about/rights_and_permissions

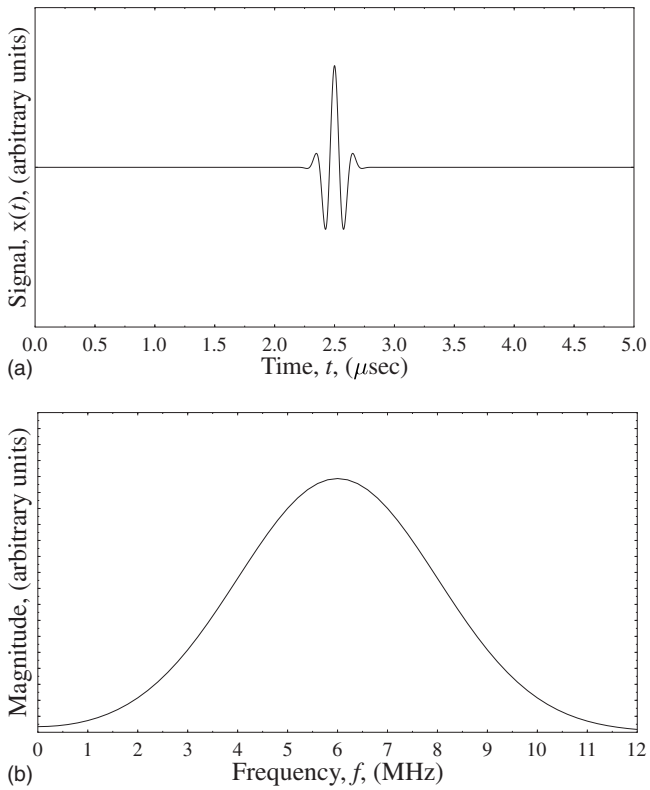

FIG. 1. (a) A wavelet generated by Eq. (5) with the center frequency f_c =6.0 MHz and bandwidth B_f=4.0 MHz. (b) Spectral distribution of the signal in the frequency domain.

$$W(a,b) = \int x(t)\bar{\psi}_{a,b}(t)dt, \tag{6}$$

where $\bar{\psi}_{a,b}(t)$ is the complex conjugate wavelet function, a is the scaling (dilation) factor, and b is the translation factor. $\bar{\psi}_{a,b}(t)$ has the form of

$$\bar{\psi}_{a,b}(t) = \frac{1}{\sqrt{a}}\psi\left(\frac{t-b}{a}\right). \tag{7}$$

In Eq. (6), $\bar{\psi}_{a,b}(t)$ corresponds to the function of $e^{j\omega t}$ in the Fourier transform. The existence of an inverse transform is confirmed only when the admissible condition is satisfied as

$$\int_{-\infty}^{\infty} \frac{\|\hat{\psi}(\omega)\|^2}{\omega} d\omega < +\infty. \tag{8}$$

Equation (6) can be written in terms of the corresponding spectrotemporal parameters such as time τ and frequency ω which represent the characteristics of the signal more intuitively in the shape of

$$W(\tau,\omega) = \int_{-\infty}^{\infty} x(t)\bar{\psi}_{\tau,\omega}(t)dt. \tag{9}$$

B. Morlet wavelet and transformation

The Morlet wavelet has a Gaussian distribution in the frequency domain,[22] and it has been known that the wavelet gives more accurate results than other wavelets since the shape of the ultrasonic excitation input is identical with the shape of the wavelet basis function. Therefore, in this paper, the Morlet wavelet is selected for both excitation function and wavelet basis. The Morlet wavelet is defined as

$$\psi(t) = e^{-j\omega_1 t}e^{-t^2/2}, \tag{10}$$

where ω_1 is the shift in frequency, and it is recommended to keep the value of $\int\psi(t)dt$ less than 10^{-6}. To keep the integration value less than the threshold, several empirical values of ω_1 have been proposed.[2] For the convenience, we adopt $\omega_1 = 2\pi$. This choice makes it easy to convert a unit from the scale number a to the engineering frequency ω. The scale value a is inversely proportional to the frequency ω as

$$a = \frac{\omega_1}{\omega}, \tag{11}$$

and ω has the unit of radian per second. Substituting Eq. (11) to Eq. (7), the wavelet function can be expressed in terms of τ and ω as

$$\psi_{\tau,\omega} = \left|\frac{\omega_1}{\omega}\right|^{-1/2}\psi\left(\frac{\omega(t-\tau)}{\omega_1}\right). \tag{12}$$

Setting the time shift t_c to be zero in Eq. (5) for the simplification, the continuous wavelet transform coefficients of the NDE signals which has the Gaussian spectrum can be expressed as

$$W(\tau,\omega) = \left|\frac{\omega_1}{\omega}\right|^{-1/2}\int_{-\infty}^{\infty} x(t)\bar{\psi}\left(\frac{\omega(t-\tau)}{\omega_1}\right)dt. \tag{13}$$

Introducing a new variable η as

$$\eta = \frac{1}{a} = \frac{\omega}{\omega_1}, \tag{14}$$

and substituting Eqs. (12) and (14) to Eq. (13), we have

$$W(\tau,\omega) = \frac{\sqrt{\eta}}{2\pi}\int_{-\infty}^{\infty} e^{h(t)}dt, \tag{15}$$

where

$$h(t) = -j\omega_c(t-t_c) - \frac{B^2(t-t_c)^2}{8} + j\omega(t-\tau) - \frac{\eta^2}{2}(t-\tau)^2. \tag{16}$$

Rearranging the terms in Eq. (16), the coefficient is simplified as

$$W(\tau,\omega) = \frac{\sqrt{\eta}}{2\pi}e^{-\gamma}\int_{-\infty}^{\infty} e^{-\alpha t^2-\beta t}dt, \tag{17}$$

where

$$\alpha = \frac{B^2+4\eta^2}{8}, \tag{18}$$

$$\beta = -j(\omega-\omega_c) - \frac{B^2 t_c + 4\eta^2\tau}{4}, \tag{19}$$

Downloaded 19 Apr 2013 to 143.248.118.125. This article is copyrighted as indicated in the abstract. Reuse of AIP content is subject to the terms at: http://jap.aip.org/about/rights_and_permissions

$$\gamma = j(\omega\tau - \omega_c t_c) + \frac{B^2 t_c^2 + 4\eta^2\tau^2}{8}. \tag{20}$$

The integration in Eq. (17) can be carried out using the known transformation

$$\int_{-\infty}^{\infty} e^{-\alpha x^2 \pm \beta x} dx = \sqrt{\frac{\pi}{\alpha}} e^{\beta^2/4\alpha}. \tag{21}$$

Then, Eq. (17) is simplified to the form of

$$W(\tau,\omega) = \sqrt{\frac{\eta}{4\pi\alpha}} e^{\beta^2/4\alpha - \gamma}. \tag{22}$$

By substituting α, β, and γ to Eq. (22), the wavelet transform of an echo is expressed as

$$W(\tau,\omega) = A(\omega) e^{\kappa(\tau,\omega)} e^{j\chi(\tau,\omega)}, \tag{23}$$

where

$$A(\omega) = \sqrt{\frac{2\eta}{\pi(B^2+4\eta^2)}} e^{-2(\omega-\omega_c)^2/(B^2+4\eta^2)}, \tag{24}$$

$$\kappa(\tau,\omega) = \frac{-B^2\eta^2}{2(B^2+4\eta^2)}(\tau - t_c)^2, \tag{25}$$

$$\chi(\tau,\omega) = \frac{4\omega_c\eta^2(t-\tau) + B^2\omega(t_c-\tau)}{B^2+4\eta^2}. \tag{26}$$

The wavelet coefficients are complex numbers, and the amplitude can be obtained by taking the absolute value as

$$|W(\tau,\omega)| = \sqrt{\frac{2\eta}{\pi(B^2+4\eta^2)}} e^{[-B^2\eta^2(\tau-t_c)^2/2(B^2+4\eta^2) - 2(\omega-\omega_c)^2/(B^2+4\eta^2)]}. \tag{27}$$

Equation (27) represents the time-frequency amplitude surface of the wavelet coefficients by using the Morlet wavelet as the mother wavelet and the input simultaneously. Along the vertical (temporal center line) axis, the value shows symmetry such that

$$|W(t_c - \Delta\tau,\omega)| = |W(t_c + \Delta\tau,\omega)|. \tag{28}$$

However, along the horizontal (frequency center line) axis, the coefficient has asymmetry as

$$|W(\tau,\omega_c - \Delta\omega)| \neq |W(\tau,\omega_c + \Delta\omega)|. \tag{29}$$

Since we have chosen $\omega_1 = 2\pi$, and the variable η can be substituted for the frequency f, Eq. (27) can be finally expressed in terms of $f = \omega/2\pi$ and $B_f = B/2\pi$ as

$$|W(\tau,f)| = \sqrt{\frac{f}{2\pi(\pi^2 B_f^2 + f^2)}} e^{[-(\pi^2 B_f^2 f^2(\tau-t_c)^2 + 4\pi^2(f-f_c)^2)/2(\pi^2 B_f^2 + f^2)]}. \tag{30}$$

The temporal resolution of the wavelet signal $W(\tau,f)$ sliced at a fixed frequency f^* can be computed from the definition as

$$\Delta_\tau = \frac{2k}{\|W(\tau,f^*)\|_2} \left\{ \int_{-\infty}^{\infty} (\tau - t_c)^2 |W(\tau,f^*)|^2 d\tau \right\}^{1/2}, \tag{31}$$

where $\|\cdot\|_2$ is the L_2-norm operator and k is a constant. By substituting Eq. (30) to Eq. (31), we have a closed-form expression for the temporal width as

$$\Delta_\tau = \left\{ 2k \left(\frac{1}{f^{*2}} + \frac{1}{\pi^2 B_f^2} \right) \right\}^{1/2}. \tag{32}$$

The value in Eq. (32) approaches to zero when the frequency f^* or the bandwidth B_f or both become larger.

III. EXAMPLES

A. Ultrasonic nondestructive signals

The pitch-catch and pulse-echo tests are the most popular techniques for nondestuctive evaluation by ultrasonic sources, and the reflected signal can be expressed in the form of[23]

$$x(t) = s(t - t_0) + \sum_{i=1}^{N} r_i s(t - t_i - t_0), \tag{33}$$

where $s(t-t_0)$ is the front face reflection, t_0 is the first arrival time, $s(t-t_i-t_0)$ are the backside reflections, r_i are the reflection coefficients, t_i are the time delays, and the subscript i denotes the index set of the reflected waves. In the pulse-echo mode, the time delay can be written as

$$t_i = \frac{2h}{c} i, \tag{34}$$

where h is the thickness of the plate, and c is the velocity of the ultrasonic wave in the tested medium. The temporal *center* and *width* of a random signal $x(t)$ can be expressed as the first moment and the second moment around the center.[24]

B. Comparison of wavelet coefficients

As shown in Fig. 1(a), a synthetic signal which has the center frequency, $f_c = 6.0$ MHz and bandwidth, $B_f = 4.0$ MHz was generated using Eq. (5). The magnitude of the frequency components is shown in Fig. 1(b). The continuous wavelet transform of the wave form in Fig. 1(a) can be obtained analytically by calculating Eq. (30). On the other hand, we can generate wavelet transform values by performing the Morlet wavelet transform numerically as described in Eq. (6).

Figure 2 shows the continuous wavelet coefficients of a pulse presented in Fig. 1(a). The amplitude in Fig. 2(a) is computed from Eq. (30) directly while the result in Fig. 2(b) is calculated by numerical integration expressed in Eq. (13). The comparison of the coefficients obtained analytically and numerically shows a good agreement in the shape and the amplitude with negligible level of noise.

C. Ultrasonic signal from a wideband transducer

We obtained a set of ultrasonic signal in the experimental configuration as illustrated in Fig. 3. A focused transducer which has the center frequency $f_c = 6.0$ MHz and the band-

Downloaded 19 Apr 2013 to 143.248.118.125. This article is copyrighted as indicated in the abstract. Reuse of AIP content is subject to the terms at: http://jap.aip.org/about/rights_and_permissions

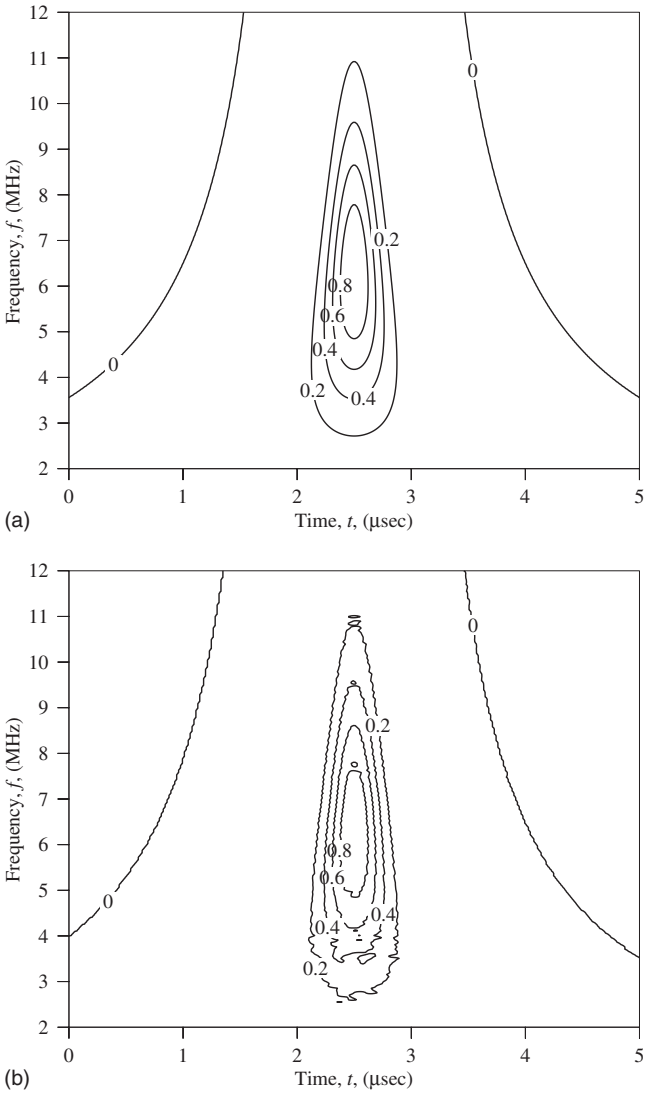

FIG. 2. Continuous wavelet transform images from a time domain signal shown in Fig. 1(a). (a) Wavelet coefficient generated by Eq. (30). (b) Wavelet coefficients numerically calculated by Eq. (6). The center frequency f_c is 6.0 MHz, and the bandwidth B_f is 4.0 MHz.

width B_f=4.0 MHz was used to send an echo and to record waves as shown in Fig. 1, and an aluminum specimen of 9.54 mm in thickness was mounted on the supports immersed in the water. The ultrasonic pulse was sent and received in the pulse-echo mode. As shown in Fig. 4(a), the received signal consists of waves reflected at the front side and the backside. The polarity of the second echo is opposite

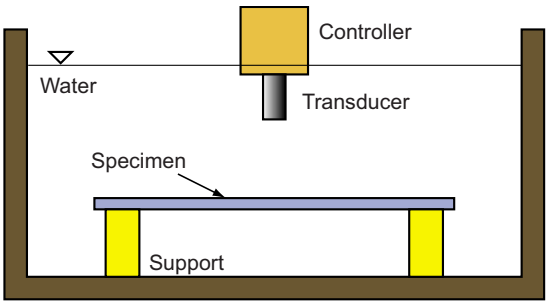

FIG. 3. (Color online) Schematic of the experimental configuration for ultrasonic immersion test.

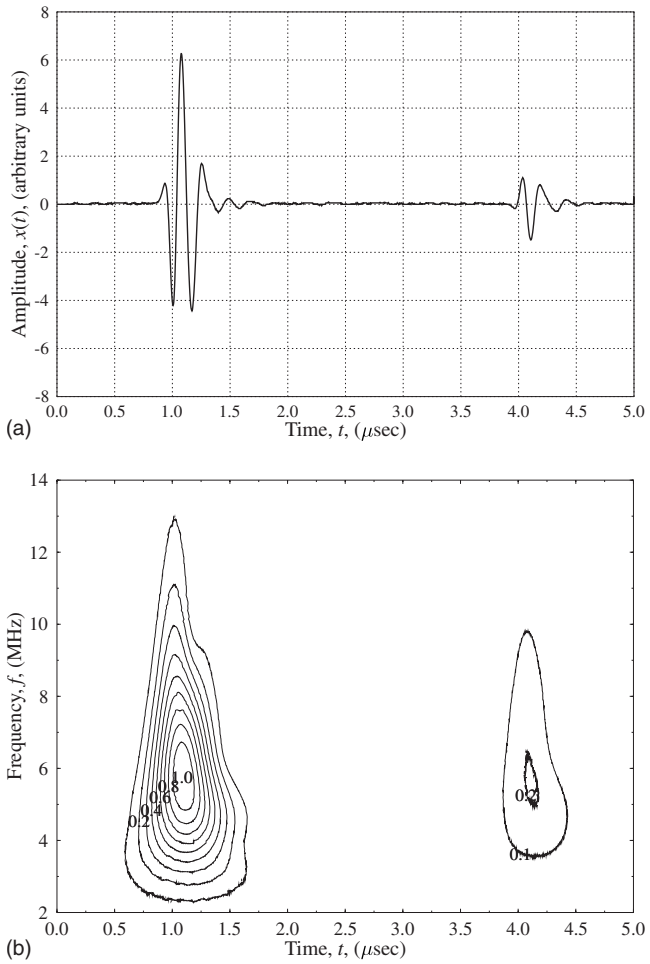

FIG. 4. Reflected waves in the experiment and wavelet representation. (a) A typical experimental wave form with the center frequency f_c=6.0 MHz and bandwidth B_f=4.0 MHz. (b) Wavelet spectrogram of the experimental signal.

to the first echo since the backside of the specimen is free in water. The amplitude of the wavelet coefficients is plotted in Fig. 4(b) by the numerical wavelet transformation. From the shapes of the plot, it is verified that the contour of Morlet wavelet coefficients has the sharp top and obtuse bottom in the spectrogram, forming a droplet like shape. The frequency of the largest amplitude in the spectrogram matches with the center frequency of the ultrasonic transducer, and the wideband signal shows the corresponding wide width along the frequency axis.

As shown in Fig. 5, the sections at different frequencies show different distributions. The temporal widths at 9.0 MHz are sharper than other peaks at other lower frequencies resulting in an improved temporal resolution due to the asymmetry aforementioned.

D. Randomly arrived signal

Cepstrum and other different techniques such as correlation method and Hilbert transformation have been widely used to decide the arrival times of ultrasonic signals.[25] However, those methods work poorly for the echoes that have irregular time differences to adjacent echoes, and the magnitude of the each echo cannot be obtained simultaneously in

Downloaded 19 Apr 2013 to 143.248.118.125. This article is copyrighted as indicated in the abstract. Reuse of AIP content is subject to the terms at: http://jap.aip.org/about/rights_and_permissions

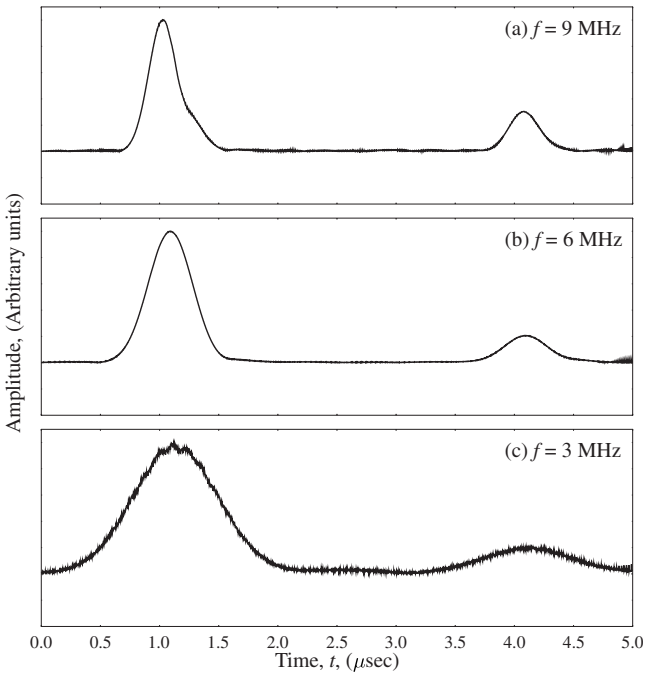

FIG. 5. Wavelet sections, cut from spectrogram in Fig. 4(b), at different frequencies: (a) f=9.0 MHz, (b) f=6.0 MHz, and (c) f=3.0 MHz.

the time-of-flight analysis. An ultrasonic signal shown in Fig. 6(a) was generated by superposing ultrasonic echoes with the magnitudes of 1.0, 0.8, 0.6, and 0.4, and the echoes are centered at 3.0 μsec, 6.0 μsec, 6.8 μsec, and 7.8 μsec, respectively.

The wavelet transformed spectrogram of the time domain signal in Fig. 6(b) was utilized for the nonlinear fitting to estimate the parameters such as magnitudes and times-of-flight using the analytical solution in Eq. (23) as a kernel function that represents the wavelet coefficients of an echo. In particular, the separable nonlinear least-squares technique[26] was used to successfully estimate the unknown parameters. In Fig. 6(c), the result of the wavelet based nonlinear fitting (WB) is compared with the cepstrum result.

IV. CONCLUSIONS AND SUMMARY

Although wavelet transformation has been widely used, the time-frequency representation has been interpreted only qualitatively. In this paper, a spectrotemporal representation of a typical ultrasonic pulse is derived and verified. The derived closed-form equation represents the water drop shape of the acoustic pulses in the wavelet domain. The quantitative comparison of the peak frequency and bandwidth verifies the wavelet representation of the derived closed-form equation. The closed-form equation is readily utilized via nonlinear least-squares optimization for estimating the number, temporal locations, and amplitudes of waves which might travel along different reflections and sources.

ACKNOWLEDGMENT

The authors wish to thank S. C. Wooh for the discussion regarding temporal resolution and A. White of the Michigan State University for providing parametric estimation result for the revision of this article.

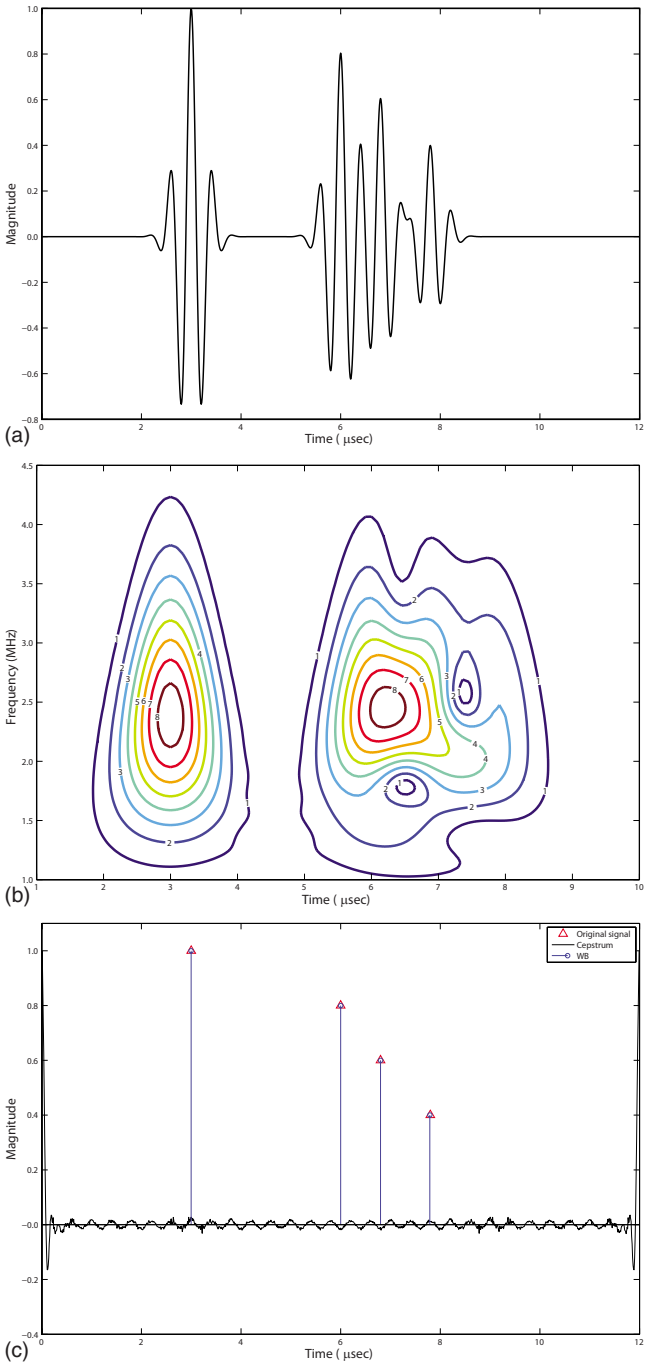

FIG. 6. (Color online) Nonlinear parameter estimation. (a) A series of ultrasonic signals which arrived with irregular time intervals, (b) wavelet representation of the ultrasonic signal, and (c) estimated time-of-flights and corresponding magnitudes by the wavelet based parameter estimation (WB) and cepstrum method (Cepstrum).

[1]G. Strang and T. Nguyen, *Wavelets and Filter Banks* (Wellesley-Cambridge Press, Wellesley, MA, 1996).
[2]A. Aldroubi, *Wavelets in Medicine and Biology* (CRC Press, Boca Raton, FL, 1996).
[3]M. Bhatia, W. Karl, and A. Willsky, IEEE Trans. Med. Imaging **15**, 92 (1996).
[4]C. H. Chen, *Time-Frequency and Time-Scale Analysis* (IEEE, Philadelphia, PA, 1994), pp. 472–475.
[5]J. Watson, P. Addison, and A. Sibbald, Shock Vib. **6**(5/6), 267 (1999).
[6]C. J. Li and J. Ma, NDT & E Int **30**(3), 143 (1997).
[7]J. Hong, Y. Kim, and H. Lee, Int. J. Solids Struct. **39**, 1803 (2002).
[8]Z. Sun and C. Chang, J. Struct. Eng. **128**, 1354 (2002).
[9]S. C. Wooh and K. Veroy, in *Review of progress in quantitative nonde-*

Downloaded 19 Apr 2013 to 143.248.118.125. This article is copyrighted as indicated in the abstract. Reuse of AIP content is subject to the terms at: http://jap.aip.org/about/rights_and_permissions

structive evaluation, Proceedings of AIP Conference, edited by D. O. Thompson and D. E. Chimenti (AIP, Melville, NY, 2000), Vol. 19, pp. 831–838.
[10]G. Qi, NDT & E Int. **33**, 133 (2000).
[11]H. Melhem and H. Kim, J. Eng. Mech. **129**, 571 (2003).
[12]S. Patsias and W. J. Staszewski, Struct. Health Monit. **1**, 5 (2002).
[13]K. Ip, P. Tse, and H. Tam, Smart Mater. Struct. **13**, 861 (2004).
[14]K. Kishimoto, H. Inoue, M. Hamada, and T. Shibuya, ASME J. Appl. Mech. **62**, 841 (1995).
[15]Y. Y. Kim and E. Kim, J. Acoust. Soc. Am. **110**, 86 (2001).
[16]S. J. Huang and C. T. Hsieh, IEEE Trans. Power Deliv. **14**, 235 (1999).
[17]J. Yang and K. Xu, J. Appl. Phys. **101**, 104902 (2007).
[18]M. Sahnoun, C. Daul, and O. Haas, J. Appl. Phys. **101**, 014911 (2007).
[19]M. Strauss, M. Sapir, M. Glinsky, and J. Melick, J. Appl. Phys. **94**, 5350 (2003).
[20]C. Wu, Ann. Stat. **9**, 501 (1981).
[21]F. Pukelsheim, *Optimal Design of Experiments* (Society for Industrial Mathematics, Philadelphia, PA, 2006).
[22]P. Goupillaud, A. Grossmann, and J. Morlet, Geoexploration **23**, 85 (1984).
[23]K. Graff, *Wave Motion in Elastic Solids* (Dover, New York, 1975).
[24]A. Papoulis, *Probability, Random Variables, and Stochastic Processes*, 3rd ed. (McGraw-Hill, New York, 1995).
[25]S. Furui, IEEE Trans. Acoust., Speech, Signal Process. **29**, 254 (1981).
[26]S. Kay, Prentice-Hall Signal Processing Series p. 595 (1993).

Downloaded 19 Apr 2013 to 143.248.118.125. This article is copyrighted as indicated in the abstract. Reuse of AIP content is subject to the terms at: http://jap.aip.org/about/rights_and_permissions